Regular Article

PHYSICAL CHEMISTRY RESEARCH
Published by the
Iranian Chemical Society
www.physchemres.org
info@physchemres.org

Phys. Chem. Res., Vol. 11, No. 4, 725-734, December 2023
DOI: 10.22036/pcr.2022.353391.2153

Molecular Analysis of Potential Inhibitors Against SARS-CoV-2: Computational Approach

C.U. Ibeji[a,b,*], G.F. Tolufashe[c,*], Z. Sanusi[b] and T.P. Omayone[d]

[a]*Department of Pure and Industrial Chemistry, Faculty of Physical Sciences, University of Nigeria, Nsukka 410001, Enugu State, Nigeria*
[b]*Catalysis and Peptide Research Unit, School of Health Sciences, University of KwaZulu-Natal, Durban 4041, South Africa*
[c]*Baruch S. Blumberg Institute, Doylestown, United States*
[d]*Department of Physiology, School of Health and Health Technology, Federal University of Technology Akure, Ondo State, Nigeria*
(Received 25 July 2022, Accepted 21 October 2022)

SARS-CoV-2 has endangered the health of notable population of the world and hence, it attracted the attention of many researchers. In this study, we introduce two potential antiviral compounds for the treatment COVID-19 and compare it with the current reference drug. Molecular dynamics simulation and quantum theory of atoms in molecules (QTAIM) were used to study the host-guest interaction and dynamics between the nCov protein and inhibitors. Results obtained after a triplicate run of 100 ns for each compound revealed that compound B2 showed better inhibitory potential with MM-GBSA binding energy of -40.05 kcal mol^{-1}, compared to the referenced drug. It is worth noting that B1 had a comparable binding potential with B2, suggesting some similarity in their inhibitory features. The QTAIM results showed that Laplacian $\nabla^2\rho(r)$ and ellipticity (ε) were positive, indicating a stable protein-ligand interaction. The order of stability was in agreement with the MM-GBSA energy trends. The results showed that B1 and B2 can be used as a hopeful therapeutic for the cure of Covid-19. Though, a crucial trial should be done to authenticate this conclusion.

Keywords: Covid-19, MMGBA, QTAIM, Antiviral compounds, SARS-CoV-2

INTRODUCTION

The coronavirus (COVID-19) infection is known as the world's pandemic infectious disease caused by a strain called SARs-CoV-2 [1]. This was revealed in 2019 in Wuhan city of China, spread all around the world, and infected more than 500 million people till July 31, 2022; it is currently a subject of concern to public health [2-4]. Developing new active drugs, in addition to available drugs under testing, is an important task for the pharmacotherapy of this disease [5-7]. Researchers are trying to find antivirals precise to the virus. Many drugs such as remdesivir (RV), chloroquine (CQ), and favipiravir are presently under clinical trials to test their efficacy and safety in the treatment of COVID-19 [8]. Targeting the spike protein has been reported as a probable strategy for treating the disease [9,10]. Therefore, an effective therapy against SARS-COV-2 needs to be discovered.

An experimental study showed that the family of 4,5-dihydro-1H-pyrrolo[3,4-c]pyrazol-6 one (pyrrolopyrazolone) binds with CA_{NTD} site 2 and prevents uncoating of viral capsids *in vitro* [11]. Two class of 4,5-dihydro-1H-pyrrolo[3,4-c]pyrazol-6 one (pyrrolopyrazolone) HIV-1 inhibitors, B1 and B2, were shown to prevent early postentry stages of viral replication. We previously studied these two inhibitors; they replicated the experimental finding and N-methylation of the inhibitors increased the chemical reactivity [12]. The coronavirus main protease has been reported to inhibit enzyme activity by blocking viral replication. This main protease has attracted much attention in drug design, including in the development

*Corresponding author. E-mail: ugochukwu.ibeji@unn.edu.ng

of effective antiviral drugs [13]. To the best of our knowledge, no work has reported the properties of these compounds for treatment of the coronavirus main protease. Since these compounds, B1 and B2, are effective against viral replication and they stop the uncoating of viral capsids *in vitro*, this work focuses on investigating the potential ability of these compounds as an antiviral therapy against the coronavirus main protease. We used computational approaches such as docking, molecular dynamics, and density functional theory to ascertain the potential of these compounds for the treatment of COVID-19 patients. We believe that our conclusions will be beneficial for the clinical management of SARS-CoV-2 patients.

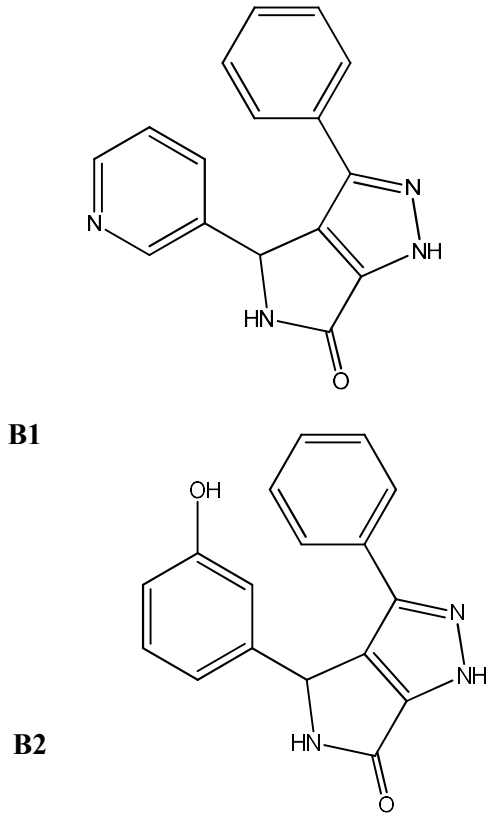

Fig. 1. 3D structural representation of B1 and B2.

COMPUTATIONAL DETAILS

Docking

The energies for the binding of B1, B2 (Fig. 1) and Chloroquine (CQ) were studied through molecular docking. 3D crystallography of SARS -CoV2 were retrieved from the protein data bank (PDB) (ID: 6M0J) [14]. AutoDock tool 1.5.4 [15] was applied to determine the appropriate grid box. The optimization of B1 and B2 was done with Gaussian 09 [16]. The dimensions were X = 26, Y = 26, and Z = 26. Grid spacing of 1.00 Å was selected. The binding site for the ligand [17,18] was determined using the Lamarckian genetic algorithm method. Gasteiger charges were added using the AutoDock tools graphical user interface implemented by MGL Tools [19]. The docking protocol was validated by re-docking the internal ligand into the binding pocket of the protein.

Molecular Dynamic Simulation

To further validate the docking protocol B1, B2 and Chloroquine were subjected to Molecular dynamics simulation. Modified molecular dynamics protocol was used as described by Ogidigo *et al.* [3] and Ibeji *et al.* [12]. The AMBER 18 software package was applied with ANTECHAMBER [20] and LEap module. FF14SB [21] force field was used for assigning protein parameters. The counter ions were added to neutralize the complex systems and the missing hydrogen atoms were added using LEap module. The TIP3P [22] was applied for suspending the systems in a water box and the particle-mesh Ewald method [23] was used for long-ranged electrostatics. The production step was completed as described previously [12]. The post-analysis was carried out using CPPTRAJ and PTRAJ modules [24]. The Radius of Gyration (RG), root mean square deviation (RMSD), root mean square deviation fluctuation (RMSF), and a triplicate run was performed on each ligand to validate the 100 ns simulation

Thermodynamic Calculations

The MM/GBSA parameter used for estimating stability and binding strength [25-27] was also determined the following protocol by Ibeji *et al.* [12]. The last 1000 frames of the 50 ns trajectory described by the following set of equations were used for averaging the binding energies.

$$E_{gas} = E_{int} + E_{vdw} + E_{ele} \quad (1)$$

$$\Delta G_{bind} = G_{complex} - G_{receptor} - G_{ligand} \quad (2)$$

$$G_{sol} = G_{GB} + G_{SA} \quad (3)$$

$$\Delta G_{bind} = E_{gas} + G_{sol} - TS \quad (4)$$

$$G_{SA} = \gamma SASA \quad (5)$$

Here, E_{gas} depicts the gas-phase energy; E_{int} is the internal energy, E_{ele} and E_{vdw} are the Coulomb and van der Waals energies, respectively. G_{sol} is the solvation free energy. Here, the polar solvation, G_{GB} contribution, is calculated by solving the GB equation and G_{SA} is the solvent-accessible surface area (SASA) calculated with the water probe radius of 1.4 Å. T and S are the temperatures and the solute entropy, respectively.

Quantum Theory of Atoms in Molecules (QTAIM)

The quantum theory of atoms in molecules is an approach employed in the investigation of bond energy and estimating its stability, which helps to analyse the bond path that occurs between an enzyme and its interacting inhibitors [28]. To describe and categorize the intramolecular hydrogen bond (HB) interactions, the last snapshots 5 ns MD were used as starting structures and were fully optimized with the DFT (B3LYP/6-31++g(d,p)) calculations. The absence or presence of an intramolecular bond critical point (BCP) defines the absence or existence of a hydrogen bond interaction. The AIM theory of Bader and Poplier [29] evaluates the significance of a chemical interaction involving hydrogen bonding. Ellipticity (ε), Laplacian of the electron density ($\nabla^2\rho(r)$) and electron density ($\rho(r)$) are calculated at the BCP [30]. Generally, the intramolecular hydrogen bond ranges from 0.002-0.040 a.u and 0.024-0.139 a.u for electron density and its Laplacian, respectively [31].A positive value of $\nabla^2\rho(r)$ at BCP indicates the electrostatic interaction and locally reduced $\rho(r)$, while a negative value of $\nabla^2\rho(r)$ indicates the covalent interaction and locally concentrated $\rho(r)$ [32].

To illustrate the intramolecular interactions formed in the complex produced from the MD simulation, an analysis of the electronic density was achieved via the AIM theory using the AIM2000 software [33]. The topology energetics of bonded atoms at BCP can be expressed as [32]:

$$\frac{1}{4}\nabla^2\rho(r_{BCP}) = 2G(r_{BCP}) + V(r_{BCP})$$

and

$$H_{BCP} = G(r_{BCP}) + V(r_{BCP})$$

The G, V and H represent the kinetic, potential, and total electronic energies, respectively. Electrostatic interaction denotes a positive total electronic charge (H) at BCP, while a negative value reveals covalent interaction. Bond ellipticity (ε) is an indicator of the stability of bonded atoms at BCP, and low ε indicates a more stable bond, which is expressed as [34];

$$\varepsilon = \left(\frac{\lambda_1}{\lambda_2} - 1\right)$$

Here, λ_1 and λ_2 denote the two negative curvatures of the density at the BCP for the X and Y principal axes. All DFT calculations were performed using Gaussian 09 [16].

RESULTS AND DISCUSSION

The spike protein for coronaviruses has attracted much attention due to the crucial role of the translated polyproteins of the viral RNA [35]. The results of the molecular docking studies revealed that the proposed antiviral compounds interacted with SARS-CoV-2 in the active site having good binding energy (Table 1). Docking protocol was further validated by re-docking with the internal ligand, resulting in RMSD less than 2 Å compared to the inhibitors.

Table 1. Binding Energies of Compounds and Standards Drug in kcal mol^{-1}

Compounds	Binding energy (kcal mol^{-1})
B1	-6.6
B2	-6.9
CQ	-5.9

CQ = Chloroquine.

To further validate the simulations, a triplicate MD simulation for each system with different starting structures

(varying initial atomic coordinates and velocities) [36] was performed (reported in supplementary information). Figure 2 showed that CQ and B1 were relatively stable during the 100ns of the MD simulation compared to B2.

From Table 2, compared to other systems, B1 displayed approximately the lowest average RMSD. The somewhat lower average RMSD of the referenced drugs is in aggrement with the reported actions of proteases [37]. The observed structural deviation may indicate the distinguishing inhibitory action of Mpro. The earlier report proposed that proteases showed a characteristic open/close mechanism of dynamic movement with enhanced binding of ligands [37]. The observed lowest structural deviation of B2, compared to B1 and chloroquine, indicates its activity to bind to the viral Mpro. Although low RMSD of B2 is a consequence of less atomic deviation, it implies the stability, based on the experimentally stated conformational/structural actions of the ligand in binding and inhibiting viral replication.

The stability of the ligand bound to the protein was measured by the ligand. From Table 2, B2 exhibited lower orientational deviation compared to the other studied ligands.

Root Mean Square Fluctuation

Root mean square fluctuations (RMSF) were analyzed to understand the feature and nature of fluctuations exhibited by the backbone atoms of the protein. During MD simulation, RMSF tells the specific conformational evolution inside the residues, which comprises secondary structure of the protein. It also displays the nature of motion and residual fluctuation. High RMSF shows higher flexibility and *visce versa*. The residues for studied systems as shown in Fig. 3 had a relatively similar form with a mixed levels of fluctuations.

The residual fluctuation of systems is shown in Table 2. The degree or nature of the residual drift from the mean positions by the key residues in the active sites plays an important role in the stabilization of the systems [12,38]. Residues 145-152
exhibited uncommon fluctuations and broader compared to other residues. ASN149 and GLY150 exhibited higher fluctuation when the ligand B2 binds at that site. Table S1 showed the RMSF values of each ligand bound at the active site residues, indicating the degree and particularity the fluctuations in these regions.

Table 2. The Calculated Average Parameters for Describing Structural Stability

Compounds	RMSD (Å)	RMSF (Å)	RoG (Å)	Ligand RMSD (Å)
B1-nCov-19	1.45	2.22	18.36	1.04
B2-nCov-19	1.39	4.22	18.30	0.46
CQ-nCov-19	1.15	2.29	18.21	1.17

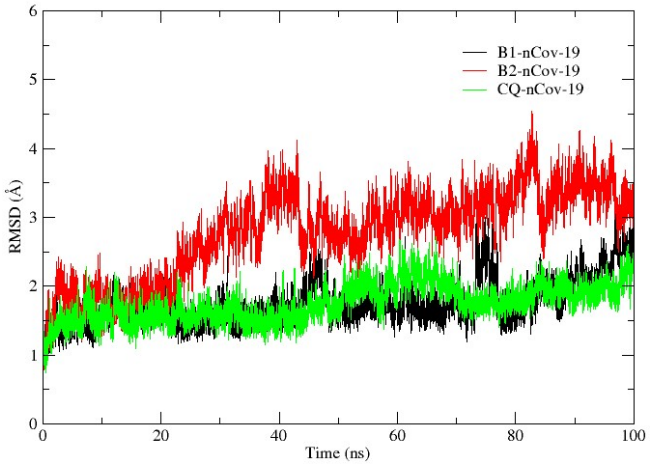

Fig. 2. RMSD plot against the time in ns during Molecular Dynamics simulation. A triplicate MD simulation for each system with different starting structures (varying initial atomic coordinates and velocities). (See supplementary)

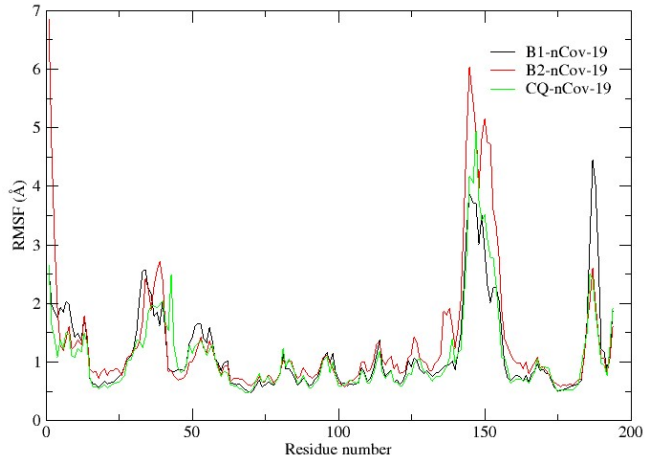

Fig. 3. Per residue fluctuation plot with the regions of interest.

Radius of Gyration

Conformation compactness. Radius of gyration (Rg) is a measure of the degree of compactness of the carbon atoms backbone of the protein. A high Rg value indicates less tightly structural packing and more mobility [12,39], and corresponds to a favourable state of the ligand binding. Figure 4 shows the structural compactness and stable conformation of studied systems and as shown in Table 2, B2 has an average Rg value of 18.3 Å that is higher compared to that of B1 and Chloroquine, suggesting a more favourable binding.

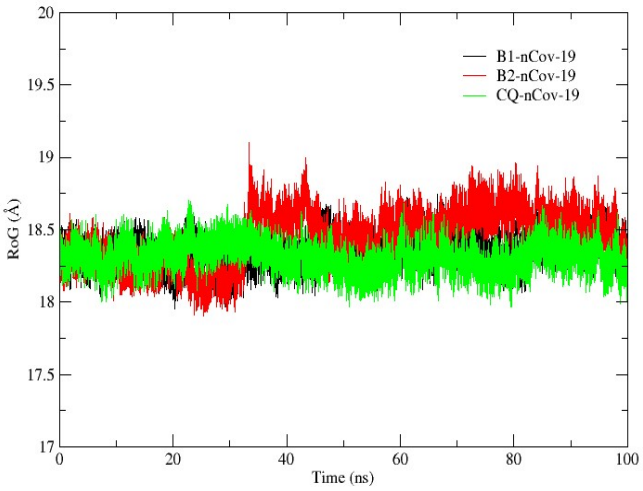

Fig. 4. The Radius of Gyration after 100 ns of the MD simulation.

MM/GBSA Calculation

The understanding of the inhibitory activity of proteases as it relates to transcription and viral replication may be channelled to design new potent anti-viral [12,38]. To examine the inhibitory potential of the compounds, compared to the reference drugs, MM/GBSA calculations were used, which is a widespread computational parameter for evaluation of the binding tendency of compounds. Table 3 shows the thermodynamic interaction of compounds with protein, suggesting the abilities of the B1 and B2 to block transcription and replication of the viral protein. The table also summarises other energy contributions such as ΔE_{ele} and ΔE_{vdw}, which characterises the electrostatic and van der Waals intermolecular components. In Table 3, the studied systems including the reference drugs show favourable binding. The MM/GBA energy presented in Table 3 for all systems revealed compound B2 as a better inhibitor with the energy value of -40.05 kcal mol^{-1} compared to that of the referenced dugs. It is interesting to note that B1 had a comparable binding affinity to B2, suggesting some similarities in their inhibitory features. This high binding affinity suggests performing further research to recognize the inimitable moieties that are responsible for high energetic interaction. CYS100 and PHE6 are displayed as crucial amino acid residues that play critical roles in the binding of compounds to Mpro, as shown in Fig. 5. According to the RMSF values corresponding to the residues, it was observed these residues perform a critical role in the conformation and binding interactions abilities of ligands with the active pockets.

A triplicate MD simulation for each system with different starting structures (varying initial atomic coordinates and velocities).

Table 3. Calculated Energies in kcal mol^{-1} and its Components Using MM-GBSA Method Obtained from the Last 1000 Snapshots of 100 ns

Compound	ΔE_{vdw}	ΔE_{ele}	ΔG_{gas}	ΔG_{polar}	$\Delta G_{nonpolar}$	$\Delta G_{solvation}$	ΔG_{bind}
B1-nCov-19	-40.60±2.87	1.79±1.71	-38.81±3.39	8.03±1.52	-4.94±0.19	3.09±1.51	-35.73±2.83
B2-nCov-19	-43.29±2.46	-2.64±1.64	-45.92±2.64	11.07±1.23	-5.19±0.19	5.88±1.28	-40.05±2.72
CQ-nCov-19	-25.05±3.54	23.14±15.24	-1.91±16.67	-14.12±14.72	-2.93±0.50	-17.05±14.48	-18.96±3.47

A triplicate MD simulation for each system with different starting structures (varying initial atomic coordinates and velocities).

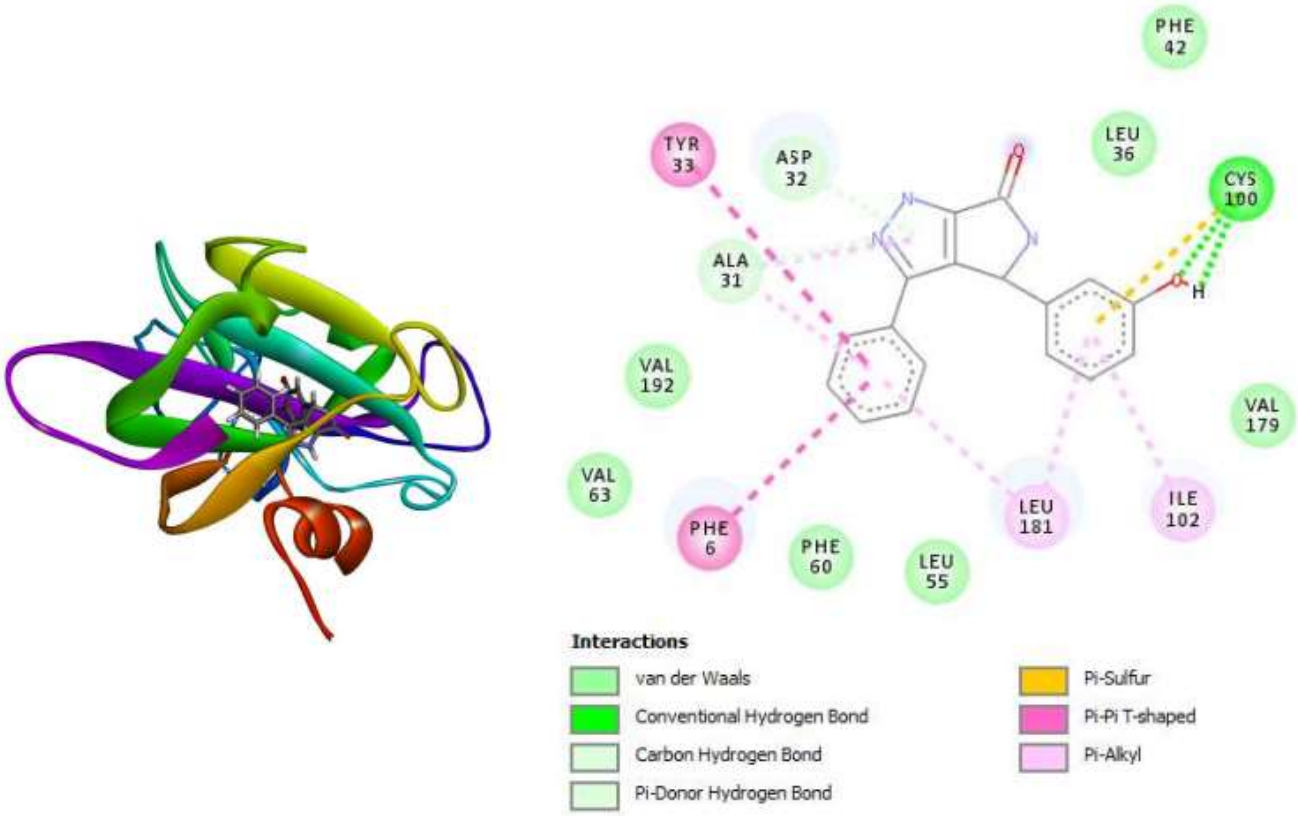

Fig. 5. 3D diagram and Residual interactions of (A) B2 (inhibitor) in complexation with nCov-19 enzyme.

QTAIM Analysis

Previous studies [40,41] have shown that the Bader and Poplier's QTAIM method is suitable for analyzing host-guest interaction [29]. The values of $\nabla^2\rho(r)$ and $\rho(r)$ are important quantum chemistry parameters for explaining charge distribution. Table 4 presents the calculated values of the $\nabla^2\rho(r)$, $\rho(r)$ and energetic parameters (G(r), V(r), H(r) and ε) at the important critical points. As earlier mentioned, a covalent (shared-shell) interaction is consistent with negative values for the Laplacian and total energy, while positive values indicates an electrostatic (closed-shell) interactions.

As can be seen from Table 4, the $\nabla^2\rho(r)$ data indicates that all interactions between the host atoms of the enzyme residues and central ions of inhibitors are closed shells. Since the ellipticity is always positive and it is used to measure the stability of the interactions, it is obvious from Table 4 that the B1 and B2 complexes not only have more HB interactions, the ε values of the most of interactions are less than 1 kcal mol^{-1}, which can indicate a more stable bond. The fact

CONCLUSIONS

In this study, two new compounds and Chloroquine were studied for a possible treatment against SARS-CoV-2. The results of the molecular dynamics and *QTAIM* approaches showed that B2 and B1 are potential inhibitors of the coronavirus with higher binding free energies compared to the reference drugs. B2 also exhibited the lowest average RMSD compared to all the studied systems. The MM-GBA showed that B2 is a better inhibitor compared to the reference dug. It is interesting to note that B1 had a comparable binding affinity toward B2, suggesting some similarity in their inhibitory features. This high binding affinity indicates the need for further research to recognize the inimitable moieties that are responsible for the high energetic interaction. From B1 possesses, the comparable binding potential and stability properties of B1 to B2 suggests a link between their inhibitory features; the both compounds can surface as a model candidates against SARS-CoV-2. The *QTAIM*

Table 4. QTAIM Topological Parameters (in a.u), Energetic Parameters V(r), G(r), and H(r) (in kcal mol^{-1}) of the Studied Complexes

Inhibitors	HB numbers	HB interactions	Electron density $\rho(r)$	Laplacian $\nabla^2\rho(r)$	V(r)	G(r)	H(r)	Ellipticity (ε)
B1-nCov-19	HB1	$H_{(lig)}$-$O_{(LEU\ 36)}$	0.0046	0.2628	0.0040	-0.0010	0.0030	0.0030
	HB2	$C_{(lig)}$-$H_{(LEU\ 36)}$	0.0071	0.0247	0.0048	-0.0014	0.0033	0.1899
	HB3	$C_{(lig)}$-$H_{(PHE\ 6)}$	0.0103	0.0348	0.0102	-0.0016	0.0054	0.3668
	HB4	$C_{(lig)}$-$C_{(PHE\ 6)}$	0.0071	0.0225	0.0045	-0.0011	0.0035	1.2003
	HB5	$H_{(lig)}$-$C_{(PHE\ 10)}$	0.0069	0.0202	0.0040	-0.0010	0.0030	0.7508
B2_covid	HB1	$N_{(lig)}$-$H_{(PHE\ 10)}$	0.0048	0.0151	0.0030	-0.0008	0.0022	0.9217
	HB2	$H_{(lig)}$-$C_{(PHE\ 6)}$	0.0067	0.0228	0.0045	-0.0011	0.0034	1.0702
	HB3	$O_{(lig)}$-$H_{(LEU\ 36)}$	0.0026	0.0097	0.0018	-0.0006	0.0012	0.0314
CQ-nCov-19	HB1	$CL_{(lig)}$-$H_{(LEU\ 36)}$	0.0080	0.0282	0.0055	-0.0015	0.0040	0.0591
	HB2	$H_{(lig)}$-$C_{(PHE\ 10)}$	0.0063	0.0245	0.0047	-0.0014	0.0033	3.3422

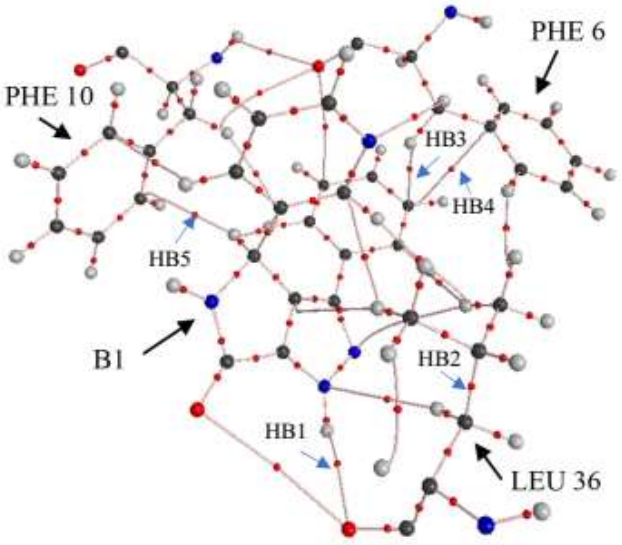

Fig. 6. Molecular graphs of B1-nCov-19 complex, showing residues (PHE 6 &10, LEU 36) in-close interaction with the B1 inhibitor. Small red dots represent the bond critical point (BCP).

analysis showed that B1 and B2 had good bond stability. These findings may provide insight into developing new treatments for SARS-COV-2.

ACKNOWLEDGEMENTS

C.U.I and ZS are thankful to CHPC (www.chpc.ac.za) for operational and infrastructural support.

REFERENCES

[1] Holshue, M. L.; DeBolt, C.; Lindquist, S.; Lofy, K.; Wiesman, J.; Bruce, H.; Spitters, C. L.; Ericson, K.; Wilkerson, S.; Tural, A.; Diaz, G. A.; Cohn, A. C.; Fox, L.; Patel, A.; Gerber, S. I.; Kim, L.; Tong, S.; Lu, X.; Lindstrom, S. E.; Pallansch, M. A.; Weldon, W. C.; Biggs, H. M.; Uyeki, T. M.; Pillai, S. K., First Case of 2019 Novel Coronavirus in the United States. *The New England J. Med.*, **2020**, *382*, 929-936. https://doi.org/10.1056/NEJMoa2001191.

[2] Wang, C.; Horby, P. W.; Hayden, F. G.; Gao, G. F., A novel coronavirus outbreak of global health concern. *Lancet*. **2020**, 15, *395* (10223), 470-473. DOI: 10.1016/S0140-6736(20)30185-9.

[3] Ogidigo, J. O.; Iwa hukuwu, E. A.; Ibeji, C. U.; Okpalefe, O.; Soliman, M. E. S., Natural phyto, compounds as possible noncovalent inhibitors against SARS-CoV2 protease: computational approach. *J. Biomol. Struct. Dyn*. **2022**. *40* (5), 2284-2301. DOI: 10.1080/07391102.2020.1837681.

[4] Barghash, R. F.; Fawzy, I. M.; Chandrasekar, V.; Singh, A. V.; Katha, U.; Mandour, A. A., *In Silico* Modeling as a Perspective in Developing Potential Vaccine Candidates and Therapeutics for COVID-19.

Coatings **2021**, *11*, 1273. https://doi.org/10.3390/coatings11111273.

[5] Harismah, K.; and M. Mirzaei, *Favipiravir: Structural Analysis and Activity against COVID-19. Adv. J. Chem. B.* **2020**, *2* (2), 55-60.

[6] Gyebi, G. A.; Ogunyemi, O. M.; Adefolalu, A. A.; López-Pastor, J. F.; Banegas-Luna, A. J.; Rodríguez-Martínez, A., *et al*. Antimalarial phytochemicals as potential inhibitors of SARS-CoV-2 guanine N7-methyltransferase (nsp 14): an integrated computational approach. *Journal of Biomolecular Structure and Dynamics.* **2022**, 1-23. DOI: 10.1080/07391102.2022.2078408.

[7] Singh, R.; Bhardwaj, V. K.; Das, P.; Purohit, R., A computational approach for rational discovery of inhibitors for non-structural protein 1 of SARS-CoV-2. *Comput. Biol. Med*. **2021**, 135, 104555. DOI: 10.1016/j.compbiomed.2021.104555.

[8] Dey, D.; Hossain, R.; Biswas, P.; Paul, P.; Islam, M.; Ema, T. I., *et al.* Amentoflavone derivatives significantly act towards the main protease (3CLPRO/MPRO) of SARS-CoV-2: *In silico* admet profiling, molecular docking, molecular dynamics simulation, network pharmacology. *Mol. Divers*. **2022**, 1-15.

[9] Jiang, S.; Lu, L.; Liu, Q.; Xu, W.; Du, L., Receptor-binding domains of spike proteins of emerging or re-emerging viruses as targets for development of antiviral vaccines. *Emerg. Microbes Infect*. **2012**, *1* (8), e13. DOI: 10.1038/emi.2012.1.

[10] Gurwitz, D., Angiotensin receptor blockers as tentative SARS-CoV-2 therapeutics. *Drug. Dev. Res*. **2020**, *81* (5), 537-540. DOI: 10.1002/ddr.21656.

[11] Lamorte, L.; Titolo, S.; Lemke, C. T.; Goudreau, N.; Mercier, J. F.; Wardrop, E.; Shah, V. B.; von Schwedler, U. K.; Langelier, C.; Banik, S. S.; Aiken, C.; Sundquist, W. I.; Mason, S. W., Discovery of novel small-molecule HIV-1 replication inhibitors that stabilize capsid complexes. *Antimicrob. Agents Chemother*. **2013**, *57* (10), 4622-4631. DOI: 10.1128/AAC.00985-13.

[12] Ibeji, C. U., Molecular dynamics and DFT study on the structure and dynamics of N-terminal domain HIV-1 capsid inhibitors. *Mol. Simul.* **2020**. *46* (1), 62-70. DOI: 10.1080/08927022.2019.1674850.

[13] Du, A.; Zheng, R.; Disoma, C.; Li, S.; Chen, Z.; Li, S., *et al.* Epigallocatechin-3-gallate, an active ingredient of Traditional Chinese Medicines, inhibits the 3CLpro activity of SARS-CoV-2. *Int. J. Biol. Macromol*. **2021**, *176*, 1-12. https://doi.org/10.1016/j.ijbiomac.2021.02.012

[14] Lan, J.; Ge, J.; Yu, J.; Shan, S.; Zhou, H.; Fan, S.; Zhang, Q.; Shi, X.; Wang, Q.; Zhang, L.; Wang, X., Structure of the SARS-CoV-2 spike receptor-binding domain bound to the ACE2 receptor. *Nature*. **2020**, *581* (7807), 215-220. DOI: 10.1038/s41586-020-2180-5.

[15] Sanner, M. F., Python: a programming language for software integration and development. *J Mol Graph Model*. **1999**, *17* (1), 57-61. PMID: 10660911.

[16] Frisch, M., *et al*., *Gaussian 09, revision D. 01*. 2009, Gaussian, Inc., Wallingford CT.

[17] Yang, B.; Hao, F.; Li, J.; Chen, D.; Liu, R., Binding of chrysoidine to catalase: spectroscopy, isothermal titration calorimetry and molecular docking studies. *J. Photochem. Photobiol. B*. **2013**, *128*, 35-42. DOI: 10.1016/j.jphotobiol.2013.08.006.

[18] Erukainure, O. L.; Ijomone, O. M.; Chukwuma, C. I.; Xiao, X.; Salau, V. F.; Islam, M. S., "Dacryodes edulis (G. Don) H.J. Lam modulates glucose metabolism, cholinergic activities and Nrf2 expression, while suppressing oxidative stress and dyslipidemia in diabetic rats". *J. Ethnopharmacol*. *255*, **2020**, 112744. DOI: 10.1016/j.jep.2022.115082.

[19] Morris, G. M.; Huey, R.; Lindstrom, W.; Sanner, M. F.; Belew, R. K.; Goodsell, D. S.; Olson, A. J., AutoDock4 and AutoDockTools4: Automated docking with selective receptor flexibility. *J. Comput. Chem*. **2009**, *30* (16), 2785-2791. DOI: 10.1002/jcc.21256.

[20] Wang, J.; Wang, W.; Kollman, P. A.; Case, D. A., Antechamber: An accessory software package for molecular mechanical calculations. *J. Am. Chem. Soc.* **2001**, *222*, 403.

[21] Perez, A.; MacCallum, J. L.; Brini, E.; Simmerling, C.; Dill, K. A., Grid-based backbone correction to the ff12SB protein force field for implicit-solvent simulations. *J. Chem. Theory Comput*. **2015**, *11* (10), 4770-4779. DOI: 10.1021/acs.jctc.5b00662.

[22] Jorgensen, W. L.; Chandrasekhar, J.; Madura, J. D.;

Impey, R. W.; Klein, M. L., Comparison of simple potential functions for simulating liquid water. *J. Chem. Phys.* **1983**, *79* (2), *926*. DOI: 10.1063/1.445869.

[23] Kholmurodov, K.; Smith, W.; Yasuoka, K.; Darden, T.; Ebisuzaki, T., A smooth-particle mesh Ewald method for DL_POLY molecular dynamics simulation package on the Fujitsu VPP700. *J. Comput. Chem.* **2000**. *21* (13), 1187-1191. DOI: 10.1002/1096-987X(200010)21:133.0.CO;2-7.

[24] Roe, D. R.; Cheatham, T., E 3rd. PTRAJ and CPPTRAJ: Software for Processing and Analysis of Molecular Dynamics Trajectory Data. *J. Chem. Theory Comput*. **2013**, *9* (7), 3084-3095. DOI: 10.1021/ct400341p.

[25] Zhou, Z.; Madura, J. D., Relative free energy of binding and binding mode calculations of HIV-1 RT inhibitors based on dock-MM-PB/GS. *Proteins*. **2004**, *57* (3), 493-503. DOI: 10.1002/prot.20223.

[26] Zhou, Z.; Wang, Y.; Bryant, S. H., Computational analysis of the cathepsin B inhibitors activities through LR-MMPBSA binding affinity calculation based on docked complex. *J. Comput. Chem*. **2009**, *30* (14), 2165-2175. DOI: 10.1002/jcc.21214.

[27] Genheden, S.; Ryde, U., The MM/PBSA and MM/GBSA methods to estimate ligand-binding affinities. *Expert. Opin. Drug Discov*. **2015**, *10* (5), 449-461. DOI: 10.1517/17460441.2015.1032936.

[28] Kheirjou, S.; Fattahi, A.; Hashemi, M. M., The intramolecular cation–π interaction of some aryl amines and its drastic influence on the basicity of them: AIM and NBO analysis. *Computational and Theoretical Chemistry*, **2014**, *1036*, 51-60. DOI: 10.1016/j.comptc.2014.02.008.

[29] Bader, R. F., Chemistry and the near-sighted nature of the one-electron density matrix. *International Journal of Quantum Chemistry.* **1995**, *56* (4), 409-419. DOI: 10.1002/qua.560560427.

[30] Mosapour-Kotena, Z.; Behjatmanesh-Ardakani, R.; Hashim, R.; Manickam-Achari, V., Hydrogen bonds in galactopyranoside and glucopyranoside: a density functional theory study. *J. Mol. Model*. **2013**, *19* (2), 589-599. DOI: 10.1007/s00894-012-1576-z.

[31] Mosapour Kotena, Z.; Behjatmanesh-Ardakani, R.; Hashim, R., AIM and NBO analyses on hydrogen bonds formation in sugar-based surfactants (α/β-d-mannose and n-octyl-α/β-d-mannopyranoside): a density functional theory study. *Liquid Crystals*. **2014**, *41* (6), 784-792. DOI: 10.1080/02678292.2014.886731.

[32] Priya, A. M.; Senthilkumar, L.; Kolandaivel, P., Hydrogen-bonded complexes of serotonin with methanol and ethanol: A DFT study. *Structural Chemistry.* **2014**, *25* (1), 139-157. DOI: 10.1007/s11224-013-0260-y.

[33] Biegler-Konig, F., *et al*., *AIM 2000, version 1; Bielefeld, Germany, 2000.*

[34] Matar, S. A.; Talib, W. H.; Mustafa, M. S.; Mubarak, M. S.; AlDamen, M. A., Synthesis, characterization, and antimicrobial activity of Schiff bases derived from benzaldehydes and 3,3′-diaminodipropylamine. *Arabian J. Chem*. **2015**. *8* (6), 850-857. DOI: 10.1016/j.arabjc.2012.12.039.

[35] Zhang, L.; Lin, D.; Sun, X.; Curth, U.; Drosten, C.; Sauerhering, L.; Becker, S.; Rox, K.; Hilgenfeld, R., Crystal structure of SARS-CoV-2 main protease provides a basis for design of improved α-ketoamide inhibitors. *Science*. **2020**, *368* (6489), 409-412. DOI: 10.1126/science.abb3405.

[36] Sabe, V. T.; Tolufashe, G. F.; Ibeji, C. U.; Maseko, S. B.; Govender, T.; Maguire, G.; Lamichhane, G.; Honarparvar, B.; Kruger, H. G., Identification of potent L,D-transpeptidase 5 inhibitors for Mycobacterium tuberculosis as potential anti-TB leads: virtual screening and molecular dynamics simulations. *J Mol Model*. **2019**, *25* (11), 328. DOI: 10.1007/s00894-019-4196-z.

[37] Munsamy, G.; Ramharack, P.; Soliman, M. E., Egress and invasion machinery of malaria: an in-depth look into the structural and functional features of the flap dynamics of plasmepsin IX and X. *RSC Advances*. **2018**, *8* (39), 21829-21840. DOI: 10.1039/C8RA04360D.

[38] Olotu, F. A.; Agoni, C.; Adeniji, E.; Abdullahi, M.; Soliman, M. E., Probing Gallate-Mediated Selectivity and High-Affinity Binding of Epigallocatechin Gallate: a Way-Forward in the Design of Selective Inhibitors for Anti-apoptotic Bcl-2 Proteins. *Appl. Biochem. Biotechnol*. **2019**, *187* (3), 1061-1080. DOI: 10.1007/s12010-018-2863-7.

[39] Emmanuel, I. A.; Olotu, F.; Agoni, C.; Soliman, M., Broadening the horizon: Integrative pharmacophore-based and cheminformatics screening of novel chemical modulators of mitochondria ATP synthase towards interventive Alzheimer's disease therapy. *Med. Hypotheses*. **2019**, *130*, 109277. DOI: 10.1016/ j.mehy.2019.109277.

[40] Djemil, R.; Attoui-Yahia, O.; Khatmi D., DFT-ONIOM study of the dopamine-β-CD complex: NBO and AIM analysis. *Canadian Journal of Chemistry*. **2015**, *93* (10), 1115-1121. DOI: 10.1139/cjc-2014-04.ss.

[41] Sanusi, Z. K.; Govender, T.; Maguire, G.; Maseko, S. B.; Lin, J.; Kruger, H. G.; Honarparvar, B., An insight to the molecular interactions of the FDA approved HIV PR drugs against L38L↑N↑L PR mutant. *J Comput Aided. Mol. Des*. **2018**, *32* (3), 459-471. DOI: 10.1007/s10822-018-0099-9.